A conditional model of local income shock and civil conflict

- Supplementary material -

Halvard Buhaug, Mihai Croicu, Hanne Fjelde & Nina von Uexkull[1]

Contents

A. DESCRIPTIVES 2
Classification of politically relevant ethnic groups 4
Construction of the *g_shock* income shock index 4
Identification of 'most likely' subsamples 5
B. VALIDATION TESTS 7
Light emission and development 10
Drought severity and local economic impact 12
C. ALTERNATIVE MODEL SPECIFICATIONS 14
Exclude influential observations 14
Moderate drought 16
Exclusion instead of discrimination 17
Expanded set of controls 18
Fixed-effects regression 19
Alternative subsamples 21
Out-of-sample cross-validation 22
D. REFERENCES 23

[1] Contact: halvard@prio.org. Replication data available via *JOP*'s Dataverse. This research has been carried out with financial support from the European Research Council, grants no. 648291 and 694640; the Research Council of Norway, grant no.168135/E10; and the Swedish Research Council, SIDA, and Formas, grant no. 2016-06389.

A. DESCRIPTIVES

Table A.1. Variable operationalizations

Name	Description	Source
Ethnic conflict onset	Outbreak of civil conflict involving group *i* in year *t*; years with ongoing conflict are truncated	Own coding based on UCDP/PRIO Armed Conflict Dataset 2016 and ACD2EPR 2014
g_shock [income shock]	Average extent of drought during all months of the growing season for the dominant local crop across all crop-producing areas of group *i*'s homeland, using the standardized precipitation evapotranspiration index (SPEI-1) with monthly negative 1.5 standard deviation as threshold for grid-level drought. The group-aggregated index has a theoretical range from 0 (no drought) to 1 (drought in all crop-producing cells in every growing-season month for group *i* in year *t*)	Own coding based on spatial agriculture production data from SPAM 2005, MIRCA and SAGE cropping calendars, gridded monthly SPEI-1 estimates from SPEIbase 2.3, and ethnic group polygons from GeoEPR 2014
Discriminated	Political discrimination of group *i* by the central state at the outset of year *t*	EPR 2014
Downgraded	Political downgrading (loss of power) of group *i* during the previous 10 years	Own coding based on EPR 2014, derived from the GROW^{UP} database
Post-Cold War	Binary indicator, years 1989–2013 = 1	Own coding
Peace years	Count of years since the previous conflict involving group *i*, logged	Own coding based on UCDP/PRIO Armed Conflict Dataset 2016 and ACD2EPR 2014
Time trend	Count of years since start of time series for group *i*	Own coding
Light emission capita	Nighttime light emission per capita for group *i* in year *t*, logged. The low local development subsample is based on group mean light emission per capita for available years, 1992–2012	Own coding based on nighttime light emission rasters from DMSP-OLS v.4, ethnic group polygons from GeoEPR 2014, and CIESIN population rasters
Ag. employment	Country-level share of workforce employed in agriculture, %. The high ag. subsample is based on median country ag. employment, 1971–2013	World Bank 2017
Cropland	Share of group *i*'s settlement area covered by cropland	Own coding based on spatial agriculture production data from SPAM 2005 and ethnic group polygons from GeoEPR 2014
Group population	Population size for group *i*, interpolated between 5-year intervals and extrapolated based on recent growth rates, logged	Own coding based on CIESIN population rasters and GeoEPR 2014 ethnic group polygons
GDP capita	Gross domestic product per capita in constant 2010 US Dollar, logged	World Bank 2017
EGIP share	Share of the country's ethnic population in power	EPR 2014
Excluded	Political exclusion of group *i* by the central state at the outset of year *t*	EPR 2014
Democracy	Polyarchy electoral democracy index (v2x)	V-Dem 6.2
Democracy sq.	Squared polyarchy index	V-Dem 6.2
Country population	Country population size, logged	World Bank 2017
Other conflict in country	Ongoing ethnic conflict in country in year *t* not involving group *i*	See ethnic conflict onset
g_shock_1.0	Similar to main indicator except using 1.0 (instead of 1.5) standard deviation as threshold for drought	See *g_shock*
c_shock	Country-aggregated drought severity indicator, derived from population-weighted averaging of *g_shock*	See *g_shock*

Dashed line separates variables included in the main models (article) from those reported only in the appendix.

Table A.2. Descriptive statistics, group-level data, 1971–2013

Variable	Obs	Mean	SD	Min	Max
Ethnic conflict onset	15,145	0.011	0.102	0	1
g_shock	15,145	0.068	0.078	0	0.8
Discriminated	15,145	0.107	0.310	0	1
Downgraded	15,145	0.089	0.285	0	1
Post-Cold War	15,145	0.610	0.488	0	1
Peace years (ln)	15,145	3.353	0.809	0	4.22
Time trend	15,145	21.27	12.31	2	44
Light emission capita (ln)[§]	7,811	0.086	0.208	0	2.587
Ag. employment[#]	5,637	26.06	22.27	0.120	82.12
Cropland	15,145	0.139	0.155	0.0002	0.810
Group population (ln)	15,145	5.996	0.899	1.861	9.017
GDP capita (ln)	13,951	7.358	1.544	3.707	11.23
EGIP share	15,145	0.784	0.253	0	1
Excluded	15,145	0.593	0.491	0	1
Democracy	15,082	0.371	0.262	0.014	0.947
Democracy sq.	15,082	0.206	0.242	0.0002	0.897
Country population (ln)	15,080	17.19	1.897	12.53	21.02
Other conflict in country	15,145	0.110	0.313	0	1
g_shock_1.0	15,145	0.191	0.129	0	0.8
N (groups)	485	-	-	-	-
N (countries)	116	-	-	-	-

Dashed line separates variables included in the main models (article) from those reported only in the appendix.
[§] 1992–2012; low development subsample defined for full 1971–2013 period based on mean group scores.
[#] 1971–2013 but with gaps; high agricultural employment subsample defined for full 1971–2013 period based on median country scores.

Table A.3. Correlation table for main variables

	Onset	*g_shock*	Discr.	Downgr.	Post-C.W.	Peace yrs	Time tr.	Light/cap
g_shock	0.011							
Discriminated	0.060	0.029						
Downgraded	0.033	-0.010	0.165					
Post-Cold War	0.023	-0.109	-0.114	-0.020				
Peace years	-0.097	-0.029	-0.079	-0.088	0.163			
Time trend	0.004	-0.074	-0.120	0.005	0.720	0.325		
Light/cap	-0.022	-0.004	0.100	-0.071	-0.004	0.079	0.005	
Ag. empl.	0.023	-0.027	-0.004	0.131	0.027	-0.134	0.028	-0.259

Classification of politically relevant ethnic groups

The Ethnic Power Relations (EPR) project (Cederman, Wimmer, and Min 2010) classifies all groups according to their status and influence on national politics, ranging from monopoly on state power to active and targeted discrimination. Two criteria define the relevant empirical sample in this study. First, we drop observations where groups enjoy 'monopoly' or 'dominant' access to central power; by definition, these groups cannot constitute the non-state challenger in an ethnic conflict against the state. Second, we focus on groups with a distinct settlement base within the territory of the host country, thus excluding dispersed, statewide, and urban groups. This selection criterion is necessary since the estimation of local income fluctuations (as described below) requires geocoded subnational settlement data in order to obtain within-country variation.[2]

The spatial delineation of ethnic groups is taken from the GeoEPR 2014 dataset (Wucherpfennig et al. 2011a). GeoEPR contains geographic information on the settlement areas of all spatially distinct ethnic groups in the EPR dataset in the form of polygon shapefiles stored in a Geographic Information System (GIS). Transnational ethnic populations, whose settlement areas span international borders, are treated as separate groups in each country. The data are time-variant, capturing significant changes in the ethnic geography and national boundaries over time, although for most groups in our sample the polygons do not change

Construction of the *g_shock* income shock index

Our variable of prime interest, *g_shock*, is a group-level drought exposure index, measured specifically for the agricultural areas within each group's ethnic homeland and specifically for the growing-season months of the locally dominant crop within each calendar year.[3] The construction of *g_shock* is based on gridded Standardized Precipitation-Evapotranspiration Index (SPEI) data, available at a spatial resolution of 0.5 decimal degrees from SPEIbase (Beguería et al. 2014; Vicente-Serrano, Beguería, and López-Moreno 2009), facilitated via PRIO-GRID (Tollefsen, Strand, and Buhaug 2012). SPEI is a superior drought indicator to the rainfall deficit measures commonly used among conflict studies, as it additionally accounts for local temperature and wind speed conditions that affect local ecology and agricultural productivity. We use the SPEI-1 index, which measures the extent of deviation in water balance for a given cell month from the long-term (1901–2013) normal SPEI condition for the same cell and month. The SPEI index is standardized and captures both positive and negative deviations. We define binary monthly grid-level drought conventionally as SPEI < -1.5; i.e., more than 1.5 standard deviations below the long-term normal (see Table C.3 results based on an alternative drought specification).

In a next step, we overlay the binary drought grid with georeferenced data on agricultural production land use, derived from the Spatial Production Allocation Model (You et al. 2014), and location-specific cropping calendar data from MIRCA (Portmann, Siebert, and Döll 2010) and SAGE (Sacks et al. 2010). From this, we estimate the prevalence of growing-season drought in each 0.5 x 0.5 degree grid cell for all years in the sample, focusing exclusively on crop-producing cells and exclusively on months that are part of the growing season for the locally dominant crop. For example, a cell that is unusually dry (SPEI < -1.5) in two out of five growing season months is assigned a local drought score, *shock*, of 0.4 for the given cell year.

[2] The statewide groups tend to enjoy monopoly or dominance on central state power; only 8% are excluded from power, compared to 48% for groups with a concentrated settlement base.

[3] Our approach is informed by von Uexkull et al. (2016), although we use a stricter classification of group-level drought that better corresponds to our theoretical argument about severe, community-wide income shocks.

Cells without agricultural production are censored, whereas cell years without observed drought are assigned a score of 0.

The extent of group-level drought exposure is then estimated by taking the arithmetic mean *shock* score of all agricultural production cells within each group's settlement area as defined by GeoEPR (Wucherpfennig et al. 2011b). The resulting *g_shock* index has a theoretical range from 0 (no drought) to 1 (drought in all cropland areas in all months of the growing season), although the maximum observed drought score is 0.8 and groups rarely experience drought scores exceeding 0.2.

Figure A.1 shows the distribution of *g_shock*. Evidently, most observations are clustered at the lower end of the scale. While this is a direct result of the rareness of severe droughts, it might introduce outlier bias, something we consider in Section C.

Figure A.1. Histogram of *g_shock*

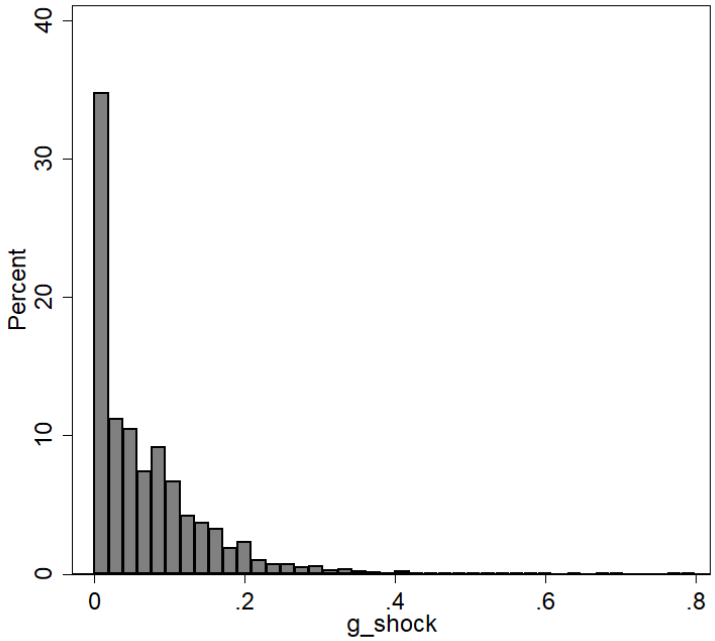

Identification of 'most likely' subsamples

The first subsample contains groups with below-median average nighttime light emission per capita, 1992–2012 (Models 2.1–2.3 in the article), which preserves those communities that are the least likely to enjoy access to technology that enhance agroeconomic resilience to growing-season drought (e.g., irrigation, early-warning systems, insurance) and have weaker economic buffers against the detrimental income effect of drought. The low local development subsample consists of 225 groups in 58 countries and is shown in Figure A.2.

The second subsample, Figure A.3, includes groups in countries where average share of the workforce employed in agriculture, 1971–2013, is above 30% (i.e., above the global mean; Models 2.4–2.6 in the article). In total, this subset contains 295 groups in 66 countries. A visual comparison of the alternative subsamples maps reveals considerable overlap despite being based on widely different types of data. Evidently, many of the least developed ethnic communities (by means of power consumption / light emission) are found in predominantly

agrarian countries, although there are also some interesting deviations between the subsamples – notably for countries with substantial intergroup inequality in nighttime light emission and power consumption.

Figure A.2. Map of low local development subsample

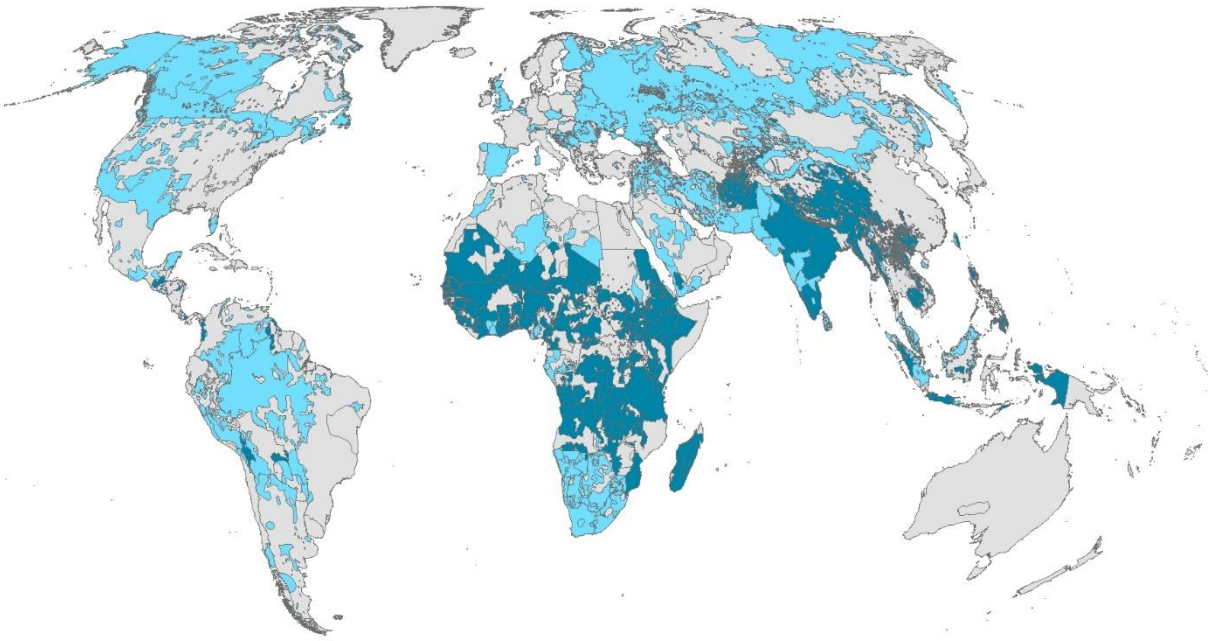

Relevant (non-monopoly nor dominant) ethnic groups with a regional base are assigned blue shades; groups with below-median average nighttime light emission per capita, 1992–2012, are shown in dark blue.

Figure A.3. Map of high agricultural employment subsample

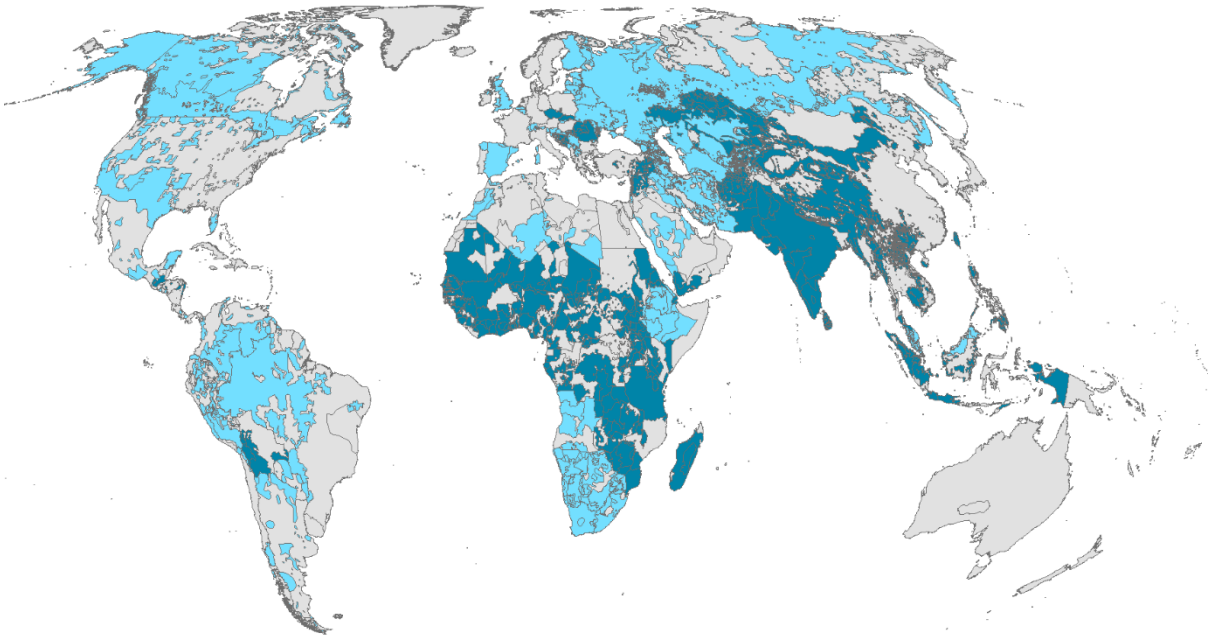

Relevant (non-monopoly nor dominant) ethnic groups with a regional base are assigned blue shades; groups in countries with at least 30% of workforce employed in agriculture are shown in dark blue.

B. VALIDATION TESTS

The merit of the analytical approach adopted in the article hinges on the assumption that a local growing-season drought has a near instant, short-term negative effect on incomes for communities dependent on agrarian livelihoods. This assumption is backed by idiosyncratic evidence but is harder to demonstrate quantitatively in a large-*N* comparative framework due to scarcity of income data at the desired level of resolution for relevant countries.

To verify that our SPEI-based *g_shock* measure still captures important dynamics in the rural economy, we conduct two validation tests. The first, documented in Table B.1, considers the association between country-aggregated drought exposure and inter-annual growth in GDP per capita. To this end, we specify *c_shock* to represent the population-weighted average *g_shock* score for all ethnic groups in each country year. We estimate a parsimonious linear regression model on two alternative samples. Each model contains three income shock terms, representing country-average drought exposure during the previous, current, and next year, respectively (the latter serving as a quasi-placebo test), in addition to time and country fixed effects. Model B1 shows the results for the global sample whereas Model B2 is limited to countries where at least 30% of the total workforce is employed in the agricultural sector on average since 1970 (WDI 2017).

In accordance with some earlier research (e.g., Miguel and Satyanath 2011), we find that severe drought exerts an instantaneous and significant negative impact on a country's production output, and the effect is especially pronounced in agriculture-dependent countries. According to Model B2, a shift from no drought to severe drought conditions results in an estimated average loss of economic growth of around 1 percentage point for agrarian societies, other factors held constant.

Table B.1. Country-level economic growth as a function of drought, 1971–2013

	(B1) *Full sample*	(B2) *Country ag. employment above 30%*
c_shock (t–1)	1.554	4.401*
	(1.458)	(2.118)
c_shock (t)	-3.979**	-5.775**
	(1.472)	(2.150)
c_shock (t+1)	-0.135	1.428
	(1.474)	(2.150)
Constant	3.156**	2.532**
	(0.553)	(0.804)
N	4,615	2,461
R^2	0.021	0.034

Note: Country and year fixed effects OLS estimates with standard errors in parentheses. * $p < 0.05$, ** $p < 0.01$. The dependent variable is interannual growth (%) in GDP per capita. *c_shock* is population-weighted average growing-season drought exposure in the country-year.

The second validation test is conducted at the theoretically more appropriate ethnic group level. Although we lack time-varying group-specific income data comparable to country GDP, remote sensing-based nighttime light imageries, which are available for the 1990s and onwards, have been shown to explain spatial variation in wealth within countries. To assess the statistical association between local growing-season drought and observable changes in local power consumption, we first calculate average annual luminosity per capita for each EPR group, 1992–2012, based on overlays of light emission rasters from the Defense Meteorological Satellite Program – Operational Linescan System (DMSP-OLS v.4) with the GeoEPR group polygons. We then measure year-on-year growth in group-level light density, expressed in percentages, similarly to the estimation of GDP per capita growth in Table B.1.

If our assumption that growing-season drought is an important driver of rural income shock is correct, and further, that nighttime light emission indeed reflects households' sensitivity to costly power consumption, we should find that *g_shock* correlates negatively and significantly with luminosity growth, all else equal. Table B.2 tests this assumption by means of group fixed effects linear regression models on three alternative samples of data: all valid ethnic groups (Model B3); groups with below-median average luminosity per capita (low development subsample, Model B4); and groups in countries with above-median employment in agriculture (agriculture-dependent subsample, Model B5). Across all three samples, we find that an increase in drought exposure is associated with a negative change in light emission growth, but the effect is much larger and more significant in the two subsamples. This gives additional evidence that growing-season drought is a reasonable proxy for local negative income deviation, although primarily for less developed and agrarian groups, where rain-fed farming and pastoralism are leading sources of livelihood.

Table B.2. Group-level light emission growth as a function of drought, 1993–2012

	(B3)	(B4)	(B5)
	Full sample	*Light emission per capita below median*	*Country ag. employment above 30%*
g_shock (t–1)	0.091	-6.214	-2.489
	(6.928)	(12.42)	(9.740)
g_shock (t)	-6.556	-27.66*	-19.83*
	(7.051)	(12.72)	(9.905)
g_shock (t+1)	1.012	20.57	0.257
	(6.997)	(12.53)	(9.772)
Time trend	-2.048**	-2.731**	-2.502**
	(0.095)	(0.177)	(0.138)
y1994	-47.13**	-55.85**	-52.65**
	(2.378)	(4.444)	(3.445)
y1997	-21.26**	-26.03**	-25.50**
	(2.199)	(4.053)	(3.198)
y2000	-5.213*	-8.812*	-6.775*
	(2.119)	(3.872)	(3.060)
y2004	7.990**	12.93**	10.91**
	(2.081)	(3.799)	(2.998)
y2010	45.47**	62.27**	54.49**
	(2.144)	(3.850)	(3.058)
Constant	71.41**	99.22**	89.54**
	(3.055)	(5.955)	(4.538)
N	7,579	3,595	4,602
R^2	0.116	0.126	0.128

Note: Group fixed effects OLS estimates with standard errors in parentheses. * $p < 0.05$, ** $p < 0.01$. The dependent variable is interannual growth (%) in group-level nighttime light emission per capita. Year dummies capture calibration noise with introduction of each new DMSP-OLS satellite.

Light emission and development

Here, we provide further justification for the use of low nighttime light emission and high share of agricultural employment as sampling criteria for identifying most-likely subsets of observations comprising poor and weather-sensitive communities. We also demonstrate why the chosen specification of *g_shock* is preferable to a more inclusive income shock proxy.

First, we show that country-aggregated nighttime light emission is strongly associated with common indicators of socioeconomic development, such as level of urbanization, log GDP per capita, and (inverse) share of population employed in agriculture (Figure B.1).

Figure B.1. Light emission vs. economic development, year 2000

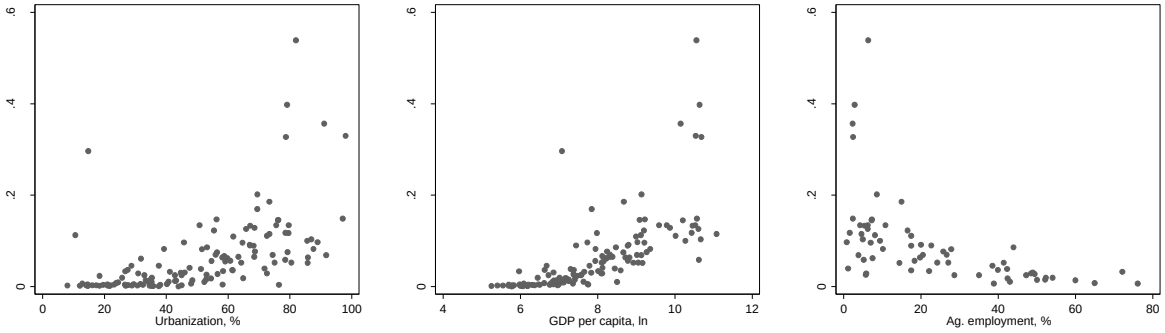

Second, we consider the association between growth rates in light emission per capita and GDP per capita. In general, light emission exhibits a much greater amplitude over time than does GDP. Of course, a considerable portion of that variation is due to measurement challenges and sheer noise; the fact that all dummies representing the introduction of new remote sensing satellites significantly explain interannual light emission growth is in itself evidence of imperfectly calibrated luminosity estimates. Even so, GDP per capita growth correlates positively and significantly with growth in light emission per capita when controlling for exogenous trends in the data (Table B.3). This suggests that light emission fluctuations do capture important economic processes and cycles in society – a pattern we argue plays out also at the community (and household) level, where average incomes fall in periods with severe droughts.

Table B.3. Light emission growth as a function of GDP growth, 1993–2012

	(B6)	(B7)
	Full sample	*Country ag. employment above 30%*
GDP capita growth (t–1)	-0.094	-0.116
	(0.088)	(0.124)
GDP capita growth (t)	0.403**	0.534**
	(0.094)	(0.135)
GDP capita growth (t+1)	-0.105	-0.052
	(0.092)	(0.135)
Time trend	-1.236**	-1.468**
	(0.074)	(0.112)
y1994	-34.34**	-38.50**
	(1.820)	(2.721)
y1997	-16.14**	-18.47**
	(1.679)	(2.534)
y2000	-3.391*	-1.974
	(1.626)	(2.456)
y2004	2.910+	7.032**
	(1.616)	(2.444)
y2010	26.94**	32.62**
	(1.736)	(2.574)
Constant	40.92**	47.87**
	(2.241)	(3.370)
N	2,498	1,346

Ordinary Least Squares (OLS) with country fixed-effects and standard errors in parentheses. $^{+}$ $p < 0.10$, * $p < 0.05$, ** $p < 0.01$. The dependent variable is interannual growth in country-aggregated light emission per capita. Although these models reveal a statistical association between GDP per capita growth and contemporaneous increases in light emission per capita, this should not be interpreted as a causal effect since private consumption (reflected by light emission) is a central component of GDP.

Drought severity and local economic impact

Third, we present a justification for the preferred specification of *g_shock*, which is a group-aggregated drought exposure measure using 1.5 standard deviations below normal meteorological conditions as the minimum threshold for classifying grid-level drought. Figure B.2 shows the distribution for an alternative income shock proxy that relies on a more inclusive threshold of just one standard deviation below median local conditions (*g_shock_1.0*). With this definition, growing-season droughts are prevalent and frequently recurring events.

We believe this specification is suboptimal as it is less able to isolate the really severe events, which plausibly could implicate widespread loss of rural incomes, from more common and manageable dry spells. The results in Table B.4 support this reasoning; Models B8–B10 show little indication that the extent of less severe droughts has an instantaneous bearing on the energy consumption among ethnic groups, in contrast to the results for more severe droughts documented in Table B.2 in the article.

Figure B.2. Histogram of *g_shock_1.0*

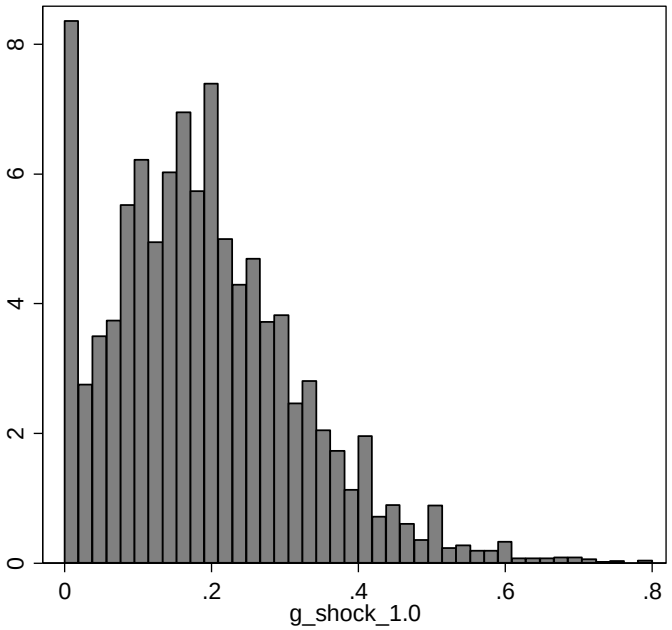

Table B.4. Group-level light emission growth as a function of *g_shock_1.0*

	(B8)	(B9)	(B10)
	Full sample	*Light emission per capita below median*	*Country ag. employment above 30%*
g_shock_1.0 (t–1)	-3.324	-7.133	-6.514
	(3.991)	(7.187)	(5.734)
g_shock _1.0 (t)	5.308	-1.018	-0.479
	(4.076)	(7.314)	(5.820)
g_shock _1.0 (t+1)	-3.778	-0.124	-7.721
	(4.071)	(7.296)	(5.819)
Time trend	-2.052**	-2.738**	-2.547**
	(0.096)	(0.181)	(0.143)
y1994	-47.09**	-55.65**	-53.44**
	(2.377)	(4.450)	(3.503)
y1997	-21.31**	-25.98**	-25.49**
	(2.199)	(4.057)	(3.258)
y2000	-5.314*	-8.616*	-7.724*
	(2.119)	(3.876)	(3.120)
y2004	7.992**	12.52**	10.71**
	(2.082)	(3.808)	(3.054)
y2010	45.64**	62.40**	55.80**
	(2.146)	(3.860)	(3.118)
Constant	71.51**	100.1**	92.34**
	(3.348)	(6.548)	(5.059)
N	7,579	3,595	4,464

Group fixed-effects Ordinary Least Squares (OLS) estimates with standard errors in parentheses. $^{+}$ $p < 0.10$, * $p < 0.05$, ** $p < 0.01$. Year dummies represent introduction of new DMSP satellite. These models are comparable to those presented in Table B.2.

C. ALTERNATIVE MODEL SPECIFICATIONS

This section presents a set of tables with altered model specifications in order to assess the robustness of main findings. We focus on the models that contain an interaction between *g_shock* and downgrading (Models 1.3, 2.3, and 2.6 in article) since this specification returned the strongest and most consistent finding across the samples and therefore constitutes the natural focal point of a sensitivity analysis. To save space, estimates for the controls – time period, time trend, and conflict history – are omitted from the table outputs below unless otherwise stated.

Exclude influential observations

As a first test, we inspect the relative importance of individual observations in shaping the coefficient estimate for the *g_shock* variable. An influential observation is commonly defined by DFBETA > $\frac{2}{\sqrt{N}}$. The five cases in Model 2.6 with the greatest influence on the estimated *g_shock* effect, listed in Table C.1, have DFBETAs scores well above the suggested threshold (equal to 0.021 in Model 2.6).[4] Unsurprisingly, these observations are all examples of ethnic conflict onset following severe drought, although none of the top-five groups were subjected to recent ethnopolitical downgrading.[5] Interestingly, we find the outbreak of the Syrian civil war on this list; a conflict that has been promoted by some as a contemporary example of a drought-driven conflict, transmitted via weather-induced loss of income and livelihood (Kelley et al. 2015; Gleick 2014; though see also Selby et al. 2017).

Table C.1. Five most influential observations on *g_shock* coefficient, Model 2.6

Country	Group	Year	Onset	*g_shock*	Downgr.	DFBETA
Sudan	Shilluk	1983	1	0.350	0	0.338
Yemen	Sunni Shafi'I	1979	1	0.429	0	0.299
Myanmar	Arakanese	1973	1	0.313	0	0.299
Senegal	Diola	2011	1	0.300	0	0.285
Syria	Sunni Arabs	2011	1	0.265	0	0.239

[4] To obtain DFBETAs for our variables of interest, we estimate the main models via country fixed-effects ordinary least squares regression. The results are comparable to our preferred mixed-effects logit models. Intuitively, one might find the DFBETA for the interaction term more informative, although excluding all observations with values above the threshold here leads to perfect prediction (no onset) for all remaining observations that experienced recent downgrading.

[5] If we let the DFBETAs for the interaction term determine the sample of outliers, we lose all groups with recent downgrading as it predicts outbreak perfectly for all observations with DFBETAs above the threshold value.

To what extent are the reported results driven by the influential cases? In Table C.2, we assess the sensitivity of the estimated income shock effect to dropping all observations with *g_shock* DFBETAs above $\frac{2}{\sqrt{N}}$. The main pattern remains much the same, with positive and significant effects for the interaction between income shock and downgraded in all three samples.

Table C.2. Excluding influential cases

	(C1)	(C2)	(C3)
	Full sample	*Light emission per capita below median*	*Country ag. employment above 30%*
g_shock (t–1)	-1.302	-1.171	0.135
	(3.242)	(3.393)	(3.369)
g_shock × Downgraded (t–1)	9.375*	10.45*	8.239+
	(4.389)	(4.672)	(4.435)
Discriminated (t–1)	1.318**	1.903**	1.689**
	(0.422)	(0.443)	(0.446)
Downgraded (t–1)	0.964+	0.540	0.934+
	(0.527)	(0.573)	(0.550)
…			
N	14,997	7,011	9,004
LR test vs. logistic (chi^2)	6.48**	4.74*	4.01*
BIC	537.5	437.4	437.8
ROC AUC	0.819	0.782	0.813

Two-level random effects logit estimates with standard errors in parentheses. $^{+}$ $p < 0.10$, * $p < 0.05$, ** $p < 0.01$. Control variables estimated but not shown. The samples exclude observations with absolute values of *g_shock* DFBETA > $\frac{2}{\sqrt{N}}$, derived from ordinary least squares regressions. Models are comparable to Models 1.3, 2.3, and 2.6, respectively.

It is reassuring that the substantive interpretation of the results is not dependent on the inclusion of influential data points. At the same time, one should not drop observations uncritically; these group years might carry special relevance and align most closely with the theoretical model. A casual inspection of the most influential cases gives us little reason to believe that they should be removed from the analysis sample. Removing a significant number of positive outcomes when group-level conflict is extremely rare also creates challenges. To illustrate, there are 160 conflict onsets (1.06%; N = 15,145) in the valid sample. Among recently downgraded groups, there are just 29 outbreaks, although the conflict rate has doubled (2.15%; N = 1,349). In the high agricultural employment subsample, this figure is further reduced to 25 conflicts (2.20%; N = 1,135). If we further limit the scope to groups with considerable drought exposure (g_shock > 0.1), we are left with just 10 conflict outbreaks (3.39%; N=295). While the increasing conflict rate with more specific subsets is exactly what the theory predicts, the diminishing number of observations makes it harder to obtain statistically significant estimates.

Moderate drought

As a third sensitivity test, we replace our standard drought index with a more inclusive operationalization of drought. Table B.4 above revealed that the alternative *g_shock_1.0* is less consistently associated with reduced luminosity growth, and therefore arguably a poorer proxy for income shock. Table C.3 shows that its effect on conflict risk also is reduced across the various samples compared to the results for the preferred *g_shock* (1.5 SD) specification, even though the general pattern is consistent with the findings discussed in main article.

Table C.3. Lower-threshold *g_shock_1.0*

	(C4)	(C5)	(C6)
	Full sample	*Light emission per capita below median*	*Country ag. employment above 30%*
g_shock _1.0 (t–1)	0.512	0.194	0.626
	(0.687)	(0.856)	(0.821)
g_shock_1.0 × Downgr. (t–1)	1.991	2.194	2.405
	(1.507)	(1.859)	(1.615)
Discriminated (t–1)	1.143**	1.248**	1.396**
	(0.218)	(0.280)	(0.265)
Downgraded (t–1)	0.212	0.156	0.192
	(0.420)	(0.501)	(0.452)
…			
N	15,145	7,096	9,096
LR test vs. logistic (chi^2)	40.07**	24.77**	26.86**
BIC	1,674.8	1,086.6	1,191.7
ROC AUC	0.873	0.852	0.840

Two-level random effects logit estimates with standard errors in parentheses. $^{+}$ $p < 0.10$, * $p < 0.05$, ** $p < 0.01$. Control variables estimated but not shown. Models are comparable to Models 1.3, 2.3, and 2.6, respectively.

Exclusion instead of discrimination

In the main article, we investigate the role of ethnopolitical discrimination, alongside downgrading, as a potential conditioning factor shaping the conflict-inducing effect of income shock (Hypothesis 2a). Discrimination implies active targeting by the central government and represents the most severe form of political exclusion with particular potential for generating collective grievances that could underpin armed mobilization, provided the right window of opportunity (Cederman, Gleditsch, and Buhaug 2013). However, since the empirical inequality literature typically uses a less restrictive classification of ethnopolitical exclusion that also includes ethnonational groups that are considered powerless or enjoying local autonomy, Table C.4 replicates the most relevant models from the main article with exclusion instead of discrimination. The results are substantively similar to those reported in Tables 1 and 2 in that there is a strong direct effect of political marginalization but at most a weak and inconsistent interaction effect with income shock.

Table C.4. Exclusion instead of discrimination as conditioning factor

	(C7)	(C8)	(C9)
	Full sample	*Light emission per capita below median*	*Country ag. employment above 30%*
g_shock (t–1)	2.081	2.346	1.747
	(1.922)	(2.109)	(2.135)
g_shock × Excluded (t–1)	-0.932	-0.821	0.147
	(2.174)	(2.446)	(2.436)
Excluded (t–1)	1.151**	1.168**	1.229**
	(0.279)	(0.337)	(0.314)
Downgraded (t–1)	0.881**	0.818**	0.945**
	(0.239)	(0.301)	(0.262)
…			
N	15,145	7,096	9,096
LR test vs. logistic (chi^2)	41.04**	15.88**	19.06**
BIC	1,676.7	1,087.1	1,191.8
ROC AUC	0.869	0.838	0.825

Two-level random effects logit estimates with standard errors in parentheses. $^{+}$ $p < 0.10$, * $p < 0.05$, ** $p < 0.01$. Control variables estimated but not shown. Models are comparable to Models 1.2, 2.2, and 2.5, respectively.

Expanded set of controls

The main results are derived from the estimation of parsimonious hierarchical two-level random effects logit models. While limiting the number of covariates has a number of positive traits, it does increase the risk of omitted variable bias. In particular, patterns of political marginalization could be affected by social and political processes not accounted for. Hence, the next set of models include a greater selection of group-specific and country-level control variables that possibly could moderate the behavior of our independent variables of primary interest (Table C.5). Unsurprisingly, some of these new controls obtain significant coefficients, but, crucially, the estimated effects of drought and political marginalization mirror those reported in the article.

Table C.5. Additional controls

	(C10)	(C11)	(C12)
	Full sample	*Light emission per capita below median*	*Country ag. employment above 30%*
g_shock (t–1)	0.384	0.892	0.655
	(1.179)	(1.408)	(1.424)
g_shock × Downgraded (t–1)	5.764*	6.664*	6.827*
	(2.595)	(2.952)	(2.780)
Discriminated (t–1)	1.086**	1.145**	1.533**
	(0.238)	(0.304)	(0.290)
Downgraded (t–1)	0.262	0.223	0.278
	(0.364)	(0.449)	(0.401)
Cropland	-1.857+	-1.176	-2.195+
	(0.958)	(1.262)	(1.154)
Group population (ln; t–1)	-0.001	-0.155	-0.047
	(0.157)	(0.210)	(0.198)
GDP capita (ln; t–1)	0.038	0.098	0.102
	(0.112)	(0.207)	(0.185)
EGIP share (t–1)	-1.395**	-0.995	-1.129+
	(0.511)	(0.613)	(0.601)
Democracy (t–1)	4.276+	2.391	3.656
	(2.249)	(3.160)	(3.075)
Democracy sq. (t–1)	-5.953*	-3.297	-4.821
	(2.544)	(3.908)	(3.781)
Country population (ln; t–1)	0.273*	0.229+	0.224+
	(0.112)	(0.132)	(0.128)
Post-Cold War	0.901**	1.063**	0.798*
	(0.288)	(0.364)	(0.336)
Peace years (ln)	-0.383**	-0.365**	-0.296**
	(0.077)	(0.101)	(0.096)
Time trend	-0.018	-0.023	-0.017
	(0.011)	(0.014)	(0.013)
Constant (group)	-8.361**	-7.167*	-7.976**
	(2.131)	(2.789)	(2.667)
Constant (country)	0.913*	0.853+	0.873*
	(0.358)	(0.514)	(0.415)
N	13,924	6,584	8,332
LR test vs. logistic (chi^2)	33.04**	13.62**	23.09**
BIC	1,542.8	1,035.1	1,127.3
ROC AUC	0.891	0.865	0.865

Two-level random effects logit estimates with standard errors in parentheses. + $p < 0.10$, * $p < 0.05$, ** $p < 0.01$. Models are comparable to Models 1.3, 2.3, and 2.6, respectively.

Fixed-effects regression

One potential concern with the main results is that there could be systematic factors unaccounted for that may be predictors of the explanatory variables and also affect the dependent variable. It is hard to find plausible candidates that influence our weather-based proxy for income shock (the SPEI index is normalized by location and thus can be considered a random treatment) but discrimination and downgrading could be sensitive to various historical and area-specific factors. Likewise, systemic changes in baseline conflict risk due to, e.g., global financial crises, oil price shocks, or major power rivalries, are not fully accounted for by the parsimonious time trend control used in the main models.

The most common causal identification strategy to avoid omitted variable bias and isolate correlates of temporal variation in Y is unit and time fixed-effects estimation (e.g., Bazzi and Blattman 2014; Dube and Vargas 2013; Miguel, Satyanath, and Sergenti 2004), although it comes at the expense of a higher risk of overfitting and lower efficiency in the absence of severe bias. For these reasons, we believe the group and year fixed-effects specification is inferior to the hierarchical random-effects model reported in the article. To remedy concerns that our results might be dependent on this assessment, we replicate the main models with linear (Table C.6) and conditional logit (Table C.7) regression containing country and year fixed-effects. Owing to the properties of logistic regression, the latter set of models exclude all groups without variation on Y (i.e., no conflict onset in the period). All models include clustered standard errors.[6] The results are in essence similar to those reported in the article.

Table C.6. OLS with group and year fixed-effects

	(C13)	(C14)	(C15)
		Light emission per capita	*Country ag. employment*
	Full sample	*below median*	*above 30%*
g_shock (t–1)	0.002	0.001	-0.002
	(0.013)	(0.020)	(0.018)
g_shock × Downgraded (t–1)	0.150^{+}	0.172	0.172^{+}
	(0.078)	(0.112)	(0.092)
Discriminated (t–1)	0.024**	0.035*	0.029*
	(0.008)	(0.014)	(0.012)
Downgraded (t–1)	0.001	-0.001	0.002
	(0.007)	(0.009)	(0.007)
…			
N	15,145	7,096	9,096
BIC	-27,356.4	-10,061.4	-14,695.2
ROC AUC	0.486	0.552	0.549

Ordinary Least Squares (OLS) estimates with group and year fixed-effects and robust standard errors, clustered on countries, in parentheses. $^{+}$ $p < 0.10$, * $p < 0.05$, ** $p < 0.01$. Control variables and year dummies estimated but not shown. Models are comparable to Models 1.3, 2.3, and 2.6, respectively.

[6] Clustered SEs are not compatible with the random effects model, reported in the article, as the hierarchical structure by design captures within-country dependence among ethnic groups.

Table C.7. Conditional logit with year fixed-effects

	(C16)	(C17)	(C18)
	Full sample	*Light emission per capita below median*	*Country ag. employment above 30%*
g_shock (t–1)	1.355	1.574	1.552
	(1.262)	(1.497)	(1.462)
g_shock × Downgraded (t–1)	6.976*	7.351*	8.540*
	(3.039)	(3.597)	(3.400)
Discriminated (t–1)	1.158**	2.073**	1.665**
	(0.475)	(0.647)	(0.592)
Downgraded (t–1)	0.434	0.312	0.551
	(0.455)	(0.551)	(0.487)
…			
N	2,772	1,853	2,151
BIC	1,073.6	800.2	848.7
ROC AUC	0.713	0.748	0.741

Conditional (group fixed-effects) logit estimates with year fixed-effects and standard errors in parentheses. $^{+}$ $p < 0.10$, * $p < 0.05$, ** $p < 0.01$. Control variables and year dummies estimated but not shown. Models are comparable to Models 1.3, 2.3, and 2.6, respectively.

Alternative subsamples

The two alternative subsamples presented in Table 2 in the main article are intended to capture the groups considered especially economically vulnerable to crop failures. At face value, these samples look reasonable (Figure A.2 and Figure A.3). Here, we consider stricter definitions of low local development and agricultural dependence, limiting the samples to groups in the lowest quartile of average nighttime light emission per capita and groups in countries where average share of workforce employed in agriculture, 1971–2013, is above 50%, respectively (Table C.8). Again, the pattern of the results is consistent with the main findings, even if statistical significance generally is weaker in the smaller samples with fewer conflicts.

Table C.8. More restrictive subsamples

	(C19) *Light emission per capita lowest quartile*	(C20) *Country ag. employment above 50%*
g_shock (t–1)	2.001	1.687
	(1.804)	(1.460)
g_shock × Downgraded (t–1)	5.037	5.574^{+}
	(3.517)	(3.081)
Discriminated (t–1)	1.967**	1.376**
	(0.337)	(0.341)
Downgraded (t–1)	0.636	0.522
	(0.478)	(0.436)
…		
N	3,511	6,655
LR test vs. logistic (chi^2)	13.05**	31.00**
BIC	627.2	855.6
ROC AUC	0.866	0.867

Two-level random effects logit estimates with standard errors in parentheses. $^{+}$ $p < 0.10$, * $p < 0.05$, ** $p < 0.01$. Control variables estimated but not shown. Models are comparable to Models 2.3 and 2.6 in the article.

Out-of-sample cross-validation

To fully explore the robustness of the reported findings and the true contribution of the *g_shock* variable to the onset model's overall performance, we conducted a set of 5-fold cross-validations. This is a hard test, particularly given the rareness of the outcome (only 160 onsets in 15,145 observations) and the complex hierarchical model. To improve stability of the simulations, we replaced the mixed-effects logit estimator with conventional logit (which produce comparable in-sample estimates). To this end, we partitioned the global sample of relevant ethnic groups into five folds of equal size, preserving the time-series structure of the data, and then sequentially created training samples consisting of four of the folds and prediction samples containing the fifth fold. We repeated this 5-fold cross-validation ten times through randomized draws, resulting in a total of 50 out-of-sample simulations.

For each iteration of the validation exercise, we estimated and then predicted three models: a conditional model that includes an interaction between income shock and downgrading (Model I below, analogous to Model 1.3), a model with income shock and downgrading as separate terms (Model II), and a baseline model without *g_shock* (Model III). The average results of these 50 cross-validation runs are listed in Table C.9 by means of area under the curve (AUC) for Receiver Operating Characteristic (ROC) and Precision-Recall (PR). For both metrics, we find that the interaction model outperforms the simpler models in correctly predicting new ethnic conflict onsets (although by a modest margin), suggesting that group-level growing-season drought captures some of the underlying data-generating process.

Table C.9. Five-fold cross-validation

Model	ROC-AUC	PR-AUC
I	0.7579	0.0362
II	0.7572	0.0348
III	0.7573	0.0351

Model I: Complete model, including interaction *g_shock* × downgraded (analogous to Model 1.3).
Model II: Same model but excluding interaction term (analogous to Model 1.1).
Model III: Baseline model, excluding *g_shock*.

D. REFERENCES

Bazzi, Samuel, and Christopher Blattman. 2014. "Economic Shocks and Conflict: Evidence from Commodity Prices." *American Economic Journal: Macroeconomics* 6 (4): 1–38.

Beguería, Santiago, Sergio M. Vicente-Serrano, Fergus Reig, and Borja Latorre. 2014. "Standardized Precipitation Evapotranspiration Index (SPEI) Revisited: Parameter Fitting, Evapotranspiration Models, Tools, Datasets and Drought Monitoring." *International Journal of Climatology* 34 (10): 3001–23.

Cederman, Lars-Erik, Kristian Skrede Gleditsch, and Halvard Buhaug. 2013. *Inequalities, Grievances, and Civil War*. Cambridge, United Kingdom: Cambridge University Press.

Cederman, Lars-Erik, Andreas Wimmer, and Brian Min. 2010. "Why Do Ethnic Groups Rebel? New Data and Analysis." *World Politics* 62 (01): 87–119.

Dube, Oeindrila, and Juan F. Vargas. 2013. "Commodity Price Shocks and Civil Conflict: Evidence from Colombia." *The Review of Economic Studies* 80 (4): 1384–1421.

Gleick, Peter H. 2014. "Water, Drought, Climate Change, and Conflict in Syria." *Weather, Climate, and Society* 6 (3): 331–40.

Kelley, Colin P., Shahrzad Mohtadi, Mark A. Cane, Richard Seager, and Yochanan Kushnir. 2015. "Climate Change in the Fertile Crescent and Implications of the Recent Syrian Drought." *Proceedings of the National Academy of Sciences* 112 (11): 3241–46.

Miguel, Edward, and Shanker Satyanath. 2011. "Re-Examining Economic Shocks and Civil Conflict." *American Economic Journal: Applied Economics* 3 (4): 228–32.

Miguel, Edward, Shanker Satyanath, and Ernest Sergenti. 2004. "Economic Shocks and Civil Conflict: An Instrumental Variables Approach." *The Journal of Political Economy* 112 (4): 725–53.

Portmann, Felix T., Stefan Siebert, and Petra Döll. 2010. "MIRCA2000—Global Monthly Irrigated and Rainfed Crop Areas around the Year 2000: A New High-Resolution Data Set for Agricultural and Hydrological Modeling." *Global Biogeochemical Cycles* 24 (1): 1–24.

Sacks, William J., Delphine Deryng, Jonathan A. Foley, and Navin Ramankutty. 2010. "Crop Planting Dates: An Analysis of Global Patterns." *Global Ecology and Biogeography* 19 (5): 607–20.

Selby, Jan, Omar S. Dahi, Christiane Fröhlich, and Mike Hulme. 2017. "Climate Change and the Syrian Civil War Revisited." *Political Geography* 60 (September): 232–44.

Tollefsen, Andreas Forø, Håvard Strand, and Halvard Buhaug. 2012. "PRIO-GRID: A Unified Spatial Data Structure." *Journal of Peace Research* 49 (2): 363–74.

Vicente-Serrano, Sergio M., Santiago Beguería, and Juan I. López-Moreno. 2009. "A Multiscalar Drought Index Sensitive to Global Warming: The Standardized Precipitation Evapotranspiration Index." *Journal of Climate* 23 (7): 1696–1718.

von Uexkull, Nina, Mihai Croicu, Hanne Fjelde, and Halvard Buhaug. 2016. "Civil Conflict Sensitivity to Growing-Season Drought." *Proceedings of the National Academy of Sciences* 113 (44): 12391–96.

WDI. 2017. *World Development Indicators 2016*. Washington, D.C.: World Bank. Retrieved December 28, 2017. (http://data.worldbank.org/data-catalog/world-development-indicators).

Wucherpfennig, Julian, Nils B. Weidmann, Luc Girardin, Lars-Erik Cederman, and Andreas Wimmer. 2011a. "Politically Relevant Ethnic Groups across Space and Time: Introducing the GeoEPR Dataset." *Conflict Management and Peace Science* 28 (5): 423–37.

———. 2011b. "Politically Relevant Ethnic Groups across Space and Time: Introducing the GeoEPR Dataset." *Conflict Management and Peace Science* 28 (5): 423–37.

You, Liangzhi, Ulrike Wood-Sichra, Steffen Fritz, Z Guo, Linda See, and J Koo. 2014. *Spatial Production Allocation Model (SPAM) 2005 Version 2.0.* Retrieved December 28, 2017. (http://mapspam.info).